

Supporting Information

DNA Photocleavage by an Osmium Complex in the PDT Window

Yujie Sun, Lauren E. Joyce, Nicole M. Dickson, and Claudia Turro*

Department of Chemistry, The Ohio State University, Columbus, OH 43210

Synthesis and characterization

[Os(bpy)₂(dppn)](PF₆)₂ (**[3]**(PF₆)₂) was synthesized by the direct coordination of dppn (35 mg) to Os(bpy)₂Cl₂^{S1} (57 mg) in refluxing 10 ml thoroughly deaerated ethylene glycol under N₂ for 4 h. The cool mixture was filtered through Celite to remove free dppn ligand. An equal volume of a saturated NH₄PF₆ solution was added to precipitate the product. The olive green solid was washed with water and ether, and dried under vacuum. Purification by chromatography on neutral alumina with acetonitrile as the eluent was applied to yield 45 mg (41 %) of the final product. ¹H NMR (400 MHz, CD₃CN; Figure S1) δ (ppm): 9.56 (dd, J = 8.16, 1.21 Hz, 2H), 9.21 (s, 2H), 8.87 (dd, J = 12.91, 8.07 Hz, 4H), 8.48 (dd, J = 5.53, 1.21 Hz, 2H), 8.45 (dd, J = 6.53, 3.22 Hz, 2H), 8.15-8.06 (m, 6H), 8.05-7.97 (m, 4H), 7.82 (dd, J = 6.67, 3.16 Hz, 2H), 7.61-7.56 (m, 2H), 7.36 (ddd, J = 7.38, 5.82, 1.30 Hz, 2H). MALDI MS: m/z, 981.2, [Os(bpy)₂(dppn)](PF₆)⁺.

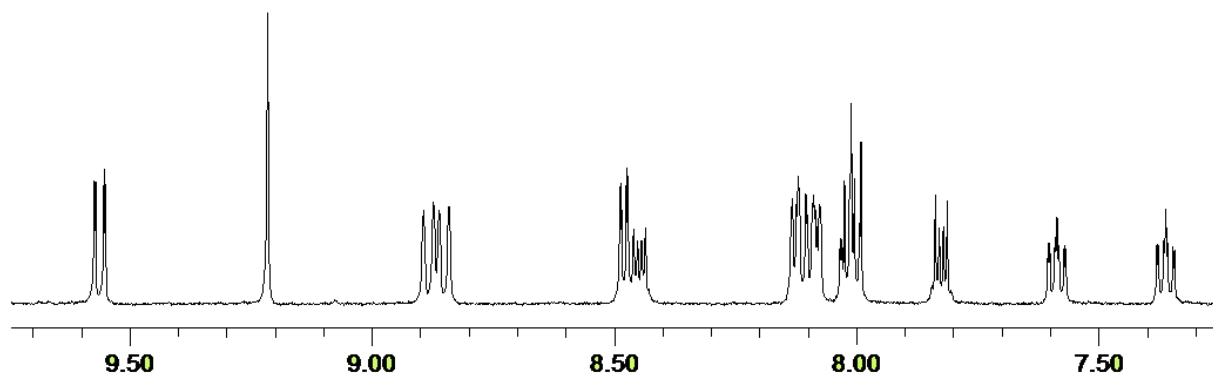


Fig. S1 ¹H NMR spectrum of [Os(bpy)₂(dppn)](PF₆)₂ in CD₃CN.

The syntheses of [Ru(bpy)₃](PF₆)₂ (**[1]**(PF₆)₂) and [Ru(bpy)₂(dppz)](PF₆)₂ (**[2]**(PF₆)₂) have been previously described.^{S2} The chloride salt of each complex was precipitated by the addition of a saturated Bu₄NCl acetone solution to the corresponding PF₆ complex in acetone. The solid was filtered, washed with acetone, diethyl ether, and dried under vacuum.

Electrochemistry

The electrochemistry of each complex was measured in a single-compartment three-electrode cell using distilled acetonitrile containing 0.1 M Bu₄NPF₆ as the supporting electrolyte, a glassy carbon working electrode, a platinum wire auxiliary electrode, and a Ag/AgCl reference electrode. At the end of each experiment, a small amount of ferrocene (Fc) was added as an internal standard, and $E_{1/2}(\text{Fc}^{+/0}) = 0.66$ V versus NHE was used as reference for calculating the oxidation and reduction potentials of each complex.^{S2}

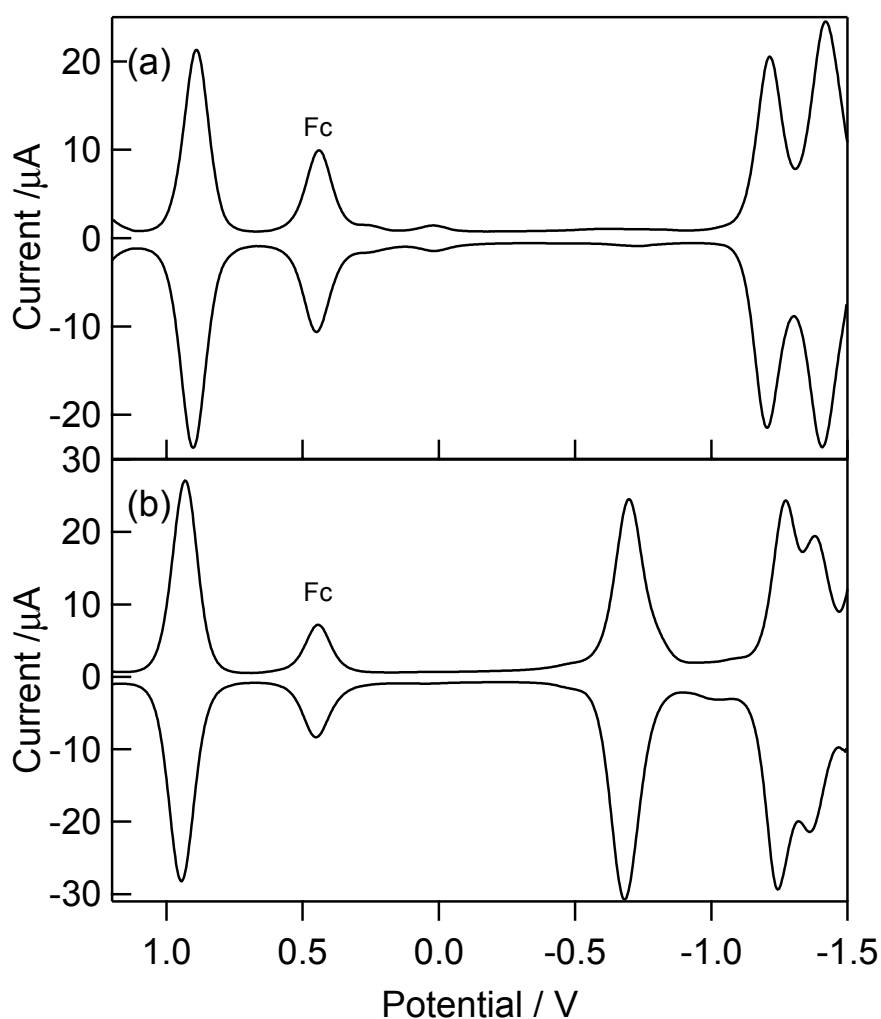


Fig. S2 Square wave voltammograms of (a) **4** and (b) **3** in CH₃CN.

Theoretical calculations

The molecular and electronic structure calculations were performed with density functional theory (DFT) using the Gaussian03 (G03) program package.^{S3} The B3LYP functional with the 6-31G** basis set^{S4} was used for hydrogen, carbon, and nitrogen. The LanL2DZ basis set^{S5} and effective core potential were for osmium. The geometries of the ground states of **3** were optimized in the gas phase with subsequent frequency analysis to show that the structures are at the local minima on the potential energy surface. Electronic structures of **3** were calculated using the conductor-like polarizable continuum model method (CPCM) with water as the solvent. Time-dependent DFT calculations produced the singlet and triplet excited states of **3** starting from its optimized singlet ground state geometry, using the CPCM method with water as the solvent. The electronic distributions and localizations were calculated using the electron density difference maps (EDDMs) by GaussSum 1.0^{S6} and the EDDM images were generated by GaussView 3.0. The electronic orbitals were visualized using Molekel 5.4.^{S7}

The calculated molecular orbital energies with corresponding orbital images of **3** are shown in Figure S3. The calculated singlet and triplet excited states of **3** are listed in Table S1 and S2, respectively.

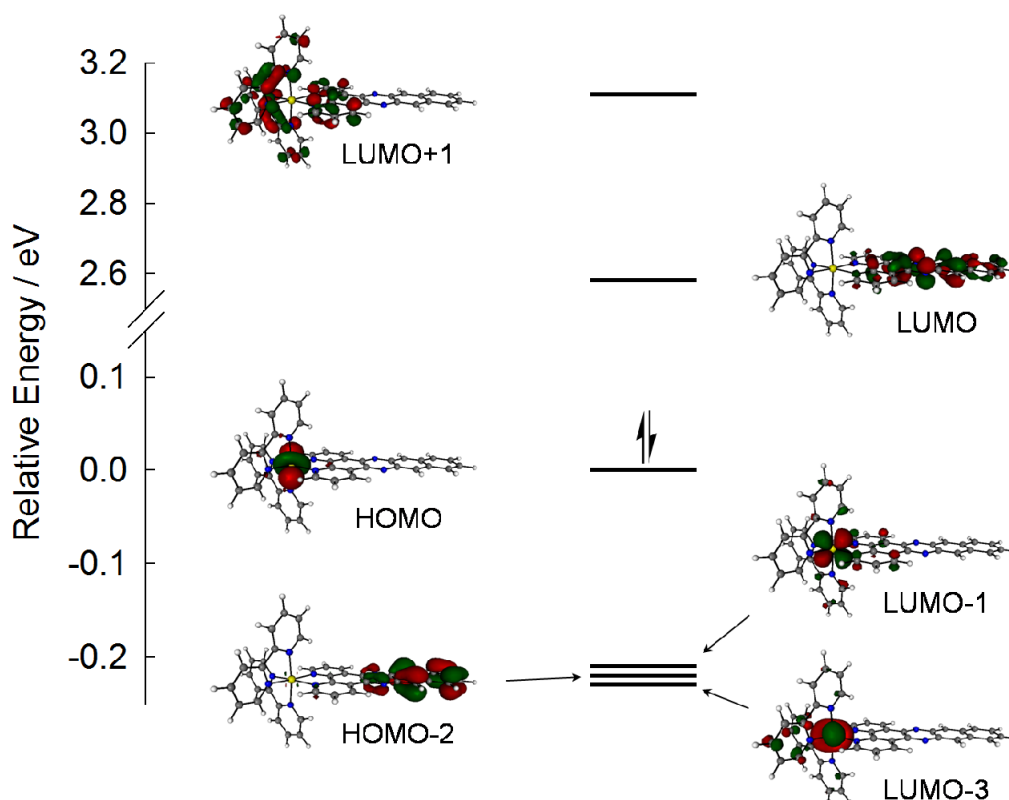


Fig. S3 Calculated MO diagram with corresponding MO pictures of **3**.

Table S1. The lowest ten calculated singlet electronic transitions with electron density difference maps (EDDMs) of **3** in water (isovalue = 0.001).

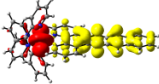
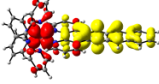
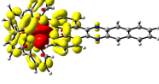
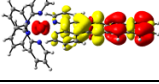
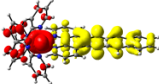
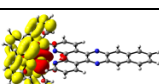
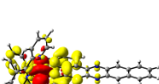
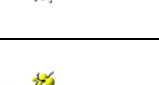
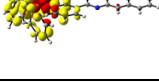
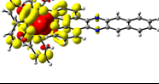
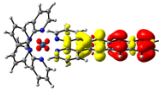
No.	E / eV	λ / nm	f	Electronic transitions (coefficient)	EDDMs
1	2.0697	599.04	0.0004	HOMO→LUMO (0.67101) HOMO→LUMO+1 (-0.16214) HOMO→LUMO+2 (0.13626)	
2	2.291	541.18	0.068	HOMO-2→LUMO (0.10611) HOMO-1→LUMO (0.68275)	
3	2.2936	540.56	0.0054	HOMO→LUMO (0.13442) HOMO→LUMO+1 (0.67322) HOMO→LUMO+2 (0.13394)	
4	2.3214	534.09	0.0205	HOMO-3→LUMO (0.16016) HOMO-2→LUMO (0.63070)	
5	2.3249	533.28	0.0005	HOMO-3→LUMO (0.66163) HOMO-3→LUMO+1 (-0.12920) HOMO-3→LUMO+2 (0.11644) HOMO-2→LUMO (-0.15300)	
6	2.3808	520.76	0.0006	HOMO→LUMO+2 (-0.11742) HOMO→LUMO+3 (0.68294)	
7	2.3959	517.48	0.0011	HOMO→LUMO (-0.16421) HOMO→LUMO+1 (-0.10130) HOMO→LUMO+2 (0.65572) HOMO→LUMO+3 (0.11523)	
8	2.576	481.31	0.0507	HOMO-3→LUMO+3 (-0.16199) HOMO-2→LUMO+1 (0.10159) HOMO-1→LUMO+1 (0.63460) HOMO-1→LUMO+2 (0.19531)	
9	2.5913	478.46	0.0312	HOMO-3→LUMO (0.11528) HOMO-3→LUMO+1 (0.62501) HOMO-1→LUMO+3 (-0.28112)	
10	2.6326	470.96	0.0052	HOMO-3→LUMO (-0.13365) HOMO-3→LUMO+1 (-0.18715) HOMO-3→LUMO+2 (0.46975) HOMO-1→LUMO+3 (-0.42973)	

Table S2. The lowest two calculated triplet electronic transitions with electron density difference maps (EDDMs) of **3** in water (isovalue = 0.001).

No.	E / eV	λ / nm	Electronic transitions (coefficient)	EDDMs
1	1.3906	891.59	HOMO-9→LUMO (-0.10811) HOMO-2→LUMO (0.79114) HOMO-2→LUMO+9 (0.19056) HOMO-1→LUMO (-0.12696)	

Transient absorption

The ultrafast transient absorption spectra were collected for each complex with a concentration of 60 – 100 μM . The samples were excited at 310 nm, with pump energy at the sample position of $\sim 6 \mu\text{J}$ (fwhm ~ 300 ps).^{S8}

The home-built transient absorption instrument for measurements on the nanosecond and microsecond timescales was previously described.^{S9} Excitation was accomplished through the use of a Spectra-Physics GCR-150 Nd:YAG laser ($\lambda_{\text{ex}} = 355$ nm, fwhm ~ 8 ns). The nanosecond transient absorption spectrum of **3** at 10 ns after laser pulse was shown in Figure S4.

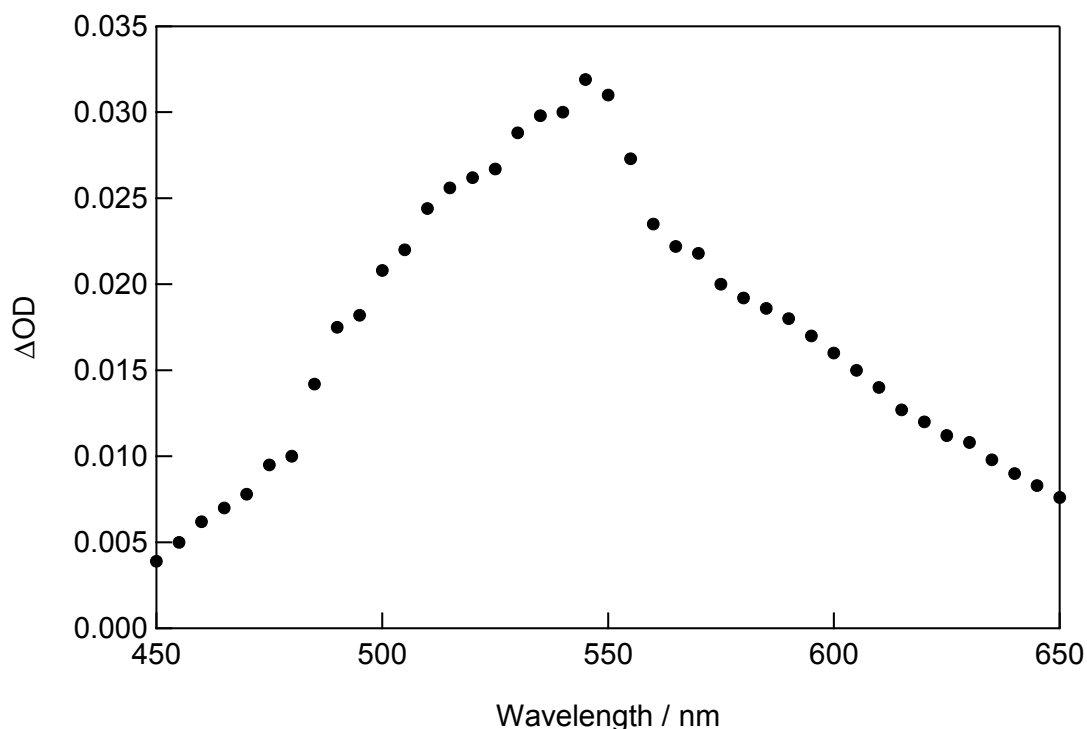


Fig. S4 Transient absorption spectrum of **3** (30 μM) in acetonitrile.

DNA photocleavage mechanism

A 150 W xenon arc lamp in a PTI housing (Milliarc Compact Lamp Housing) powered by an LPS-220 power supply (PTI) with an LPS-221 igniter (PTI) was used as the irradiation source for the DNA photocleavage experiments. The irradiation wavelength was selected by placing long-pass colored glass filters (Melles Griot) between the source and the sample. The ethidium bromide stained agarose gels were imaged using a GelDoc 2000 transilluminator (BioRad) equipped with Quantity One (version 4.0.3) software.

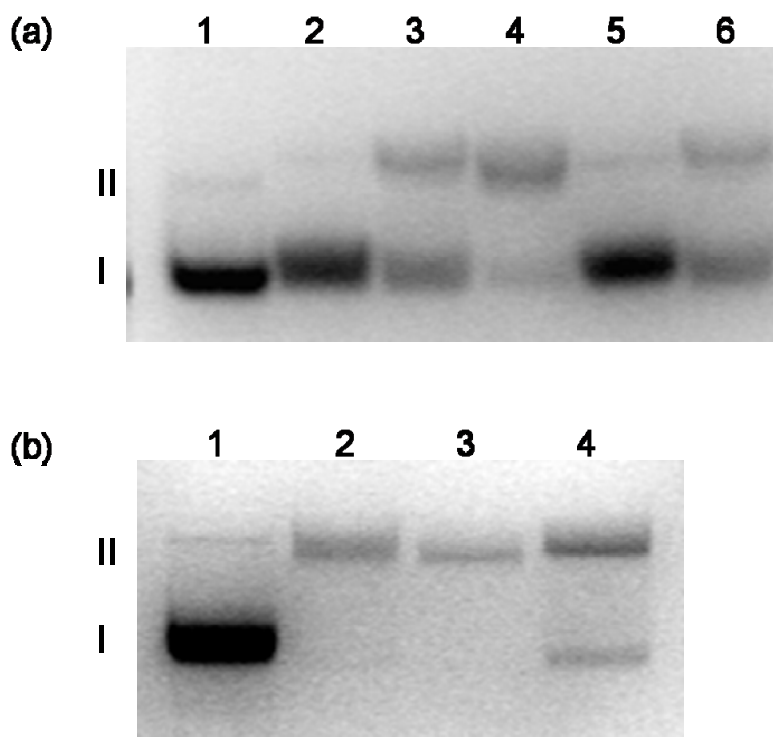


Figure S5. Ethidium bromide stained agarose gel of the photocleavage of 100 μM pUC18 plasmid by 20 μM **3** in 5 mM Tris with 50 mM NaCl (pH = 7.5) at (a) $t_{\text{irr}} = 60$ min, $\lambda_{\text{irr}} \geq 495$ nm. Lane 1 contains plasmid only in dark. Lanes 2 – 6 with both of complex and plasmid were irradiated under various conditions. Lane 2, dark; lane 3, in air; lane 4, in D_2O ; lane 5, six freeze-pump-thaw cycles; lane 6, 2 units superoxide dismutase. (b) $t_{\text{irr}} = 60$ min, $\lambda_{\text{irr}} \geq 455$ nm. Lane 1 contains DNA only. Lanes 2 – 4 with both of complex and plasmid were irradiated under various conditions. Lane 2, in air; lane 3, in D_2O ; and lane 4, 50mM NaN_3 .

References

- S1 E. M. Kober, J. V. Caspar, B. P. Sullivan and T. J. Meyer, *Inorg. Chem.*, 1988, **27**, 4587.
- S2 Y. Sun, D. A. Lutterman and C. Turro, *Inorg. Chem.*, 2008, **47**, 6427.
- S3 C.; Millam, J. M.; Iyengar, S. S.; Tomasi, J.; Barone, V.; Mennucci, B.; Cossi, M.; Scalmani, G.; Rega, N.; Petersson, G. A.; Nakatsuji, H.; Hada, M.; Ehara, M.; Toyota, K.; Fukuda, R.; Hasegawa, J.; Ishida, M.; Nakajima, T.; Honda, Y.; Kitao, O.; Nakai, H.; Klene, M.; Li, X.; Knox, J. E.; Hratchian, H. P.; Cross, J. B.; Bakken, V.; Adamo, C.; Jaramillo, J.; Gomperts, R.; Stratmann, R. E.; Yazyev, O.; Austin, A. J.; Cammi, R.; Pomelli, C.; Ochterski, J. W.; Ayala, P. Y.; Morokuma, K.; Voth, G. A.; Salvador, P.; Dannenberg, J. J.; Zakrzewski, V. G.; Dapprich, S.; Daniels, A. D.; Strain, M. C.; Farkas, O.; Malick, D. K.; Rabuck, A. D.; Raghavachari, K.; Foresman, J. B.; Ortiz, J. V.; Cui, Q.; Baboul, A. G.; Clifford, S.; Cioslowski, J.; Stefanov, B. B.; Liu, G.; Liashenko, A.; Piskorz, P.; Komaromi, I.; Martin, R. L.; Fox, D. J.; Keith, T.; Al-Laham, M. A.; Peng, C. Y.; Nanayakkara, A.; Challacombe, M.; Gill, P. M. W.; Johnson, B.; Chen, W.; Wong, M. W.; Gonzalez, C.; Pople, J. A., *Gaussian 03, revision C.02*, Gaussian, Inc.; Wallingford, CT, 2004.
- S4 A. D. McLean and G. S. Chandler, *J. Chem. Phys.*, 1980, **72**, 5639.
- S5 P. J. Hay and W. R. Wadt, *J. Chem. Phys.*, 1985, **82**, 270.
- S6 N. M. O'Boyle and J. G. Vos, *GaussSum 1.0*, Dublin City University, 2005; available at <http://gausssum.sourceforge.net>.
- S7 *Varetto U. <MOLEKEL Version>; Swiss National Supercomputing Centre: Manno (Switzerland)*.
- S8 G. Burdzinski, J. C. Hackett, J. Wang, T. L. Gustafson, C. M. Hadad and M. S. Platz, *J. Am. Chem. Soc.*, 2006, **128**, 13402.
- S9 J. T. Warren, W. Chen, D. H. Johnston and C. Turro, *Inorg. Chem.*, 1999, **38**, 6187.